Development 140, 4070-4080 (2013) doi:10.1242/dev.099838

The neogenin/DCC homolog UNC-40 promotes BMP signaling via the RGM protein DRAG-1 in *C. elegans*

Chenxi Tian[1,*], Herong Shi[1], Shan Xiong[2], Fenghua Hu[1,3], Wen-Cheng Xiong[2] and Jun Liu[1,‡]

SUMMARY

The deleted in colorectal cancer (DCC) homolog neogenin functions in both netrin- and repulsive guidance molecule (RGM)-mediated axon guidance and in bone morphogenetic protein (BMP) signaling. How neogenin functions in mediating BMP signaling is not well understood. We show that the sole *C. elegans* DCC/neogenin homolog UNC-40 positively modulates a BMP-like pathway by functioning in the signal-receiving cells at the ligand/receptor level. This function of UNC-40 is independent of its role in netrin-mediated axon guidance, but requires its association with the RGM protein DRAG-1. We have identified the key residues in the extracellular domain of UNC-40 that are crucial for UNC-40–DRAG-1 interaction and UNC-40 function. Surprisingly, the extracellular domain of UNC-40 is sufficient to promote BMP signaling, in clear contrast to the requirement of its intracellular domain in mediating axon guidance. Mouse neogenin lacking the intracellular domain is also capable of mediating BMP signaling. These findings reveal an unexpected mode of action for neogenin regulation of BMP signaling.

KEY WORDS: BMP signaling, Neogenin, DCC, UNC-40, RGM, DRAG-1, *Caenorhabditis elegans*

INTRODUCTION

The development of multicellular organisms requires the proper spatial and temporal coordination of many intracellular and extracellular signals. Among the extracellular signals are the bone morphogenetic proteins (BMPs), which belong to the transforming growth factor-β (TGFβ) superfamily of ligands. BMPs regulate a variety of developmental processes (Wu and Hill, 2009). Malfunction of this pathway causes many somatic and hereditary disorders in humans, including skeletal abnormalities, cardiovascular diseases and cancer (Gordon and Blobe, 2008; Massagué, 2008; Cai et al., 2012). Activation of the canonical BMP pathway starts with the formation of the BMP ligand-type I-type II receptor ternary complex, which in turn leads to the phosphorylation of the receptor-regulated Smads (R-Smads). These activated R-Smads then complex with common-mediator Smads (co-Smads), enter the nucleus and complex with transcriptional co-factors to regulate downstream gene expression (Shi and Massagué, 2003).

Owing to the diverse functions of the BMP pathway, multiple factors act as modulators to ensure proper spatiotemporal control of BMP signaling (Balemans and Van Hul, 2002; Umulis et al., 2009; Huang and Chen, 2012; Ramel and Hill, 2012). The transmembrane protein neogenin is one such factor. Neogenin is a member of the deleted in colorectal cancer (DCC) family and serves as a receptor for the guidance cue netrin (Keino-Masu et al., 1996) and the repulsive guidance molecules (RGMs) (Cole et al., 2007; Rajagopalan et al., 2004) to regulate axon guidance. Recent studies have shown that neogenin also plays a role in modulating BMP signaling (Zhang et al., 2009; Lee et al., 2010; Zhou et al., 2010). However, how neogenin modulates BMP signaling is not well understood. Outstanding questions include whether it acts in the signal-producing cell or the signal-receiving cell, whether its role in BMP signaling is mediated through binding or processing RGM proteins, and whether its roles in mediating BMP signaling and netrin signaling are independent processes (Tian and Liu, 2013). In this study, we provide evidence that UNC-40, the single neogenin/DCC homolog in *C. elegans*, positively promotes the BMP-like Sma/Mab (Small/Male tail abnormal) pathway and that this function is independent of its role in netrin signaling. Moreover, we found that UNC-40 functions in the signal-receiving cells by interacting with the sole RGM protein DRAG-1 to promote BMP signaling. We have identified the critical residues in UNC-40 involved in the interaction with DRAG-1. Our results also demonstrated that the extracellular domain of UNC-40 is sufficient to mediate BMP signaling and that this mode of action is conserved in mammals.

MATERIALS AND METHODS

C. elegans strains

Analyses were performed at 20°C unless otherwise noted. The following mutations and integrated transgenes were used. Linkage group I (LG I): *drag-1(jj4)*; *unc-40(e1430)*; *unc-40(tr115)*; *unc-40(ev457)*; *unc-40(ev495)*; *unc-40(jj59)*; *unc-40(e271)*; *mec-4::gfp (zdIs5)*. LG II: *sma-6(jj6)*. LG III: *lon-1(jj67), sma-3(jj3), ccIs4438(intrinsic CC::gfp)*. LG IV: *unc-5(e53)*. LG V: *dbl-1(wk70)*. LG X: *lon-2(e678)*; *sma-9(cc604)*; *unc-6(ev400)*.

Plasmid constructs and transgenic lines

Constructs for tissue-specific expression of *unc-40*, mammalian cell culture expression, DRAG-1 and UNC-40 vertebrate and *C. elegans* hybrid construction, and for *in vivo* structure-function analysis of UNC-40 are listed in supplementary material Table S1. pJKL449 (*myo-2p::gfp::unc-54 3′UTR*) was used as a co-injection marker for generating all the extrachromosomal array-containing transgenic lines.

All the *drag-1* expressing constructs (supplementary material Table S1) were in the pCFJ151 plasmid backbone, which allows insertion into the ttTi5605 Mos site (Frøkjaer-Jensen et al., 2008). The *drag-1* portion in these constructs was derived from pCXT183 (*3.9kb drag-1p::drag-1 genomic sequence without 3rd intron::gfp::1.7kb drag-1 3′UTR*), which was a

[1]Department of Molecular Biology and Genetics, Cornell University, Ithaca, NY 14853, USA. [2]Institute of Molecular Medicine and Genetics and Department of Neurology, Medical College of Georgia, Georgia Regents University, Augusta, GA 30912, USA. [3]Weill Institute of Molecular and Cell Biology, Cornell University, Ithaca, NY 14853, USA.

*Present address: Koch Institute for Integrative Cancer Research, Massachusetts Institute of Technology, Cambridge, MA 02139, USA
‡Author for correspondence (JL53@cornell.edu)

Accepted 24 July 2013

derivative of pJKL849 (Tian et al., 2010) with sequences corresponding to the third intron of *drag-1* deleted. MosSCI single-copy insertion lines were generated using the direct gonadal injection method following the protocol described (Frøkjaer-Jensen et al., 2008). Primer pairs CXT310 (GCGGGATCATTTCTTACTAG)/CXT226 (ACTGACGAATTCCCTGAATTTGTAAATACTCTTC) and CXT312 (CAAGGACTTGGATAAATTGGC)/CXT311 (GTGTATCTGCATTAACCAATA) were used to verify the insertion in different transgenic lines.

Body size measurement

Hermaphrodite animals at the gravid adult stage were collected and treated with hypochlorite. The resulting embryos were allowed to hatch in M9 buffer at 16°C. Synchronized L1s were plated onto NGM plates and allowed to grow for 48 or 72 hours before they were washed off the plates, treated with 0.3% sodium azide, and mounted onto 2% agarose pads. Images of the worms were taken on a Leica DMRA2 compound microscope with a Hamamatsu Orca-ER camera using Openlab software (Improvision). To overcome the slow growth phenotype of certain mutant strains, animals whose vulva development was at the early Christmas tree stage were used for body size measurement in certain experiments. Subsequent statistical analyses were performed using Microsoft Excel.

RAD-SMAD reporter assay

Hermaphrodites carrying the RAD-SMAD reporter *jjIs2437* II (Tian et al., 2010) were treated with hypochlorite. The resulting embryos were allowed to hatch in M9 buffer at 16°C. Synchronized L1s were plated onto NGM plates and allowed to grow for 48 hours. The resulting L3 animals were anesthetized. Images of the hypodermal cells were taken at 40× magnification on a Leica DMRA2 compound microscope. Fluorescence intensity of the nuclear GFP and background was measured in pairs using the Openlab software. Five nuclei/background pairs were measured for each worm. A total of 40 worms was measured per genotype. The mean signal value of each worm was deduced by averaging nuclear signal minus background signal. Standard deviation was then calculated using Microsoft Excel.

Assays to evaluate the Unc phenotypes of *unc-40* mutants

Synchronized L1s were plated onto NGM plates and allowed to grow for different lengths of time. Forty-eight hours post-plating, the AVM neuronal migration defect was determined by examining AVM axon projection using the *mec-4::gfp (zdIs5)* marker (Clark and Chiu, 2003). Animals that failed to project the AVM axon ventrally were considered abnormal (supplementary material Fig. S1). The movement defect was determined by visually inspecting the movement of animals 72 hours post-plating. The wild type-like moving animals were given a score of 1 and the animals that rarely moved or moved in an extremely uncoordinated fashion upon stimulation were given a score of 4. The egg-laying defective (Egl) phenotype was determined at 100 hours post-plating by counting the number of animals that died as a 'bag of worms' due to defective egg laying.

Immunofluorescence staining

Animal fixation, immunostaining, microscopy and image analysis were performed as described previously (Tian et al., 2010). Guinea pig anti-FOZI-1 (1:200) (Amin et al., 2007), mouse monoclonal anti-AJM-1 MH27 (1:100; Developmental Studies Hybridoma Bank, University of Iowa), rat anti-MLS-2 (1:200) (Jiang et al., 2005) and goat anti-GFP (1:1000; Rockland Immunochemicals) were used.

Cell culture and transient transfection

HEK293T cells (for co-immunoprecipitation experiments), HEK293 cells (for BMP assays) and primary skin fibroblasts were maintained in Dulbecco's Modified Eagle Medium supplemented with 10% fetal calf serum and 100 units/ml penicillin G and streptomycin (Gibco). HEK293 or HEK293T cells were transfected by the calcium phosphate method as described previously (Lee et al., 2010). Primary fibroblasts were plated at a density of 10^6 cells per 10-cm culture dish and allowed to grow for 24-48 hours before transfection using Lipofectamine 2000 (Invitrogen). Forty-eight hours after transfection, cells were washed, serum starved overnight, and then treated with BMP2 (30 minutes for HEK293 cells and 60 minutes for fibroblasts). Cells were then subjected to western blot or luciferase assay analyses, respectively. Alternatively, cell media or cell lysates were collected for co-immunoprecipitation assays as described below.

Luciferase assay

Luciferase assay was carried out as described previously (Zhou et al., 2010). In brief, cells were washed with PBS and lysed in lysis buffer (Promega) for 20 minutes at room temperature. Then, 50 µl of lysate were used to determine relative luciferase activity (firefly luciferase activity divided by Renilla luciferase activity) using a dual luciferase assay system (Promega). The luciferase activity data are the average of two independent cell isolations, each performed in triplicate.

Co-immunoprecipitation assays

For proteins that were expressed as soluble proteins, including mutated and wild-type Myc-FN5,6, DRAG-1 (mature domain)-FLAG, DRAG-1 (mature domain)-Myc and FLAG-DBL-1 (mature domain), cell media were collected 5 days after transfecting the corresponding protein-expressing plasmids. For the remaining proteins, including mutated and wild-type DRAG-1 (mature domain)-FLAG, Myc-SMA-6 and Myc-DAF-4, cell lysates were collected 48 hours post-transfection. Anti-cMyc-conjugated Sepharose beads (Sigma EzView; 8 µl beads per reaction) or anti-FLAG-conjugated Sepharose beads (Sigma M2 EzView; 6 µl per reaction) were first incubated with cell lysates or media containing the first protein for 4 hours at 4°C, then with cell lysates or media containing the second protein for 4 hours or overnight at 4°C. The beads were then subjected to five washes with lysis buffer (50 mM Tris pH 8.0, 150 mM NaCl, 1% Triton X-100), boiled in SDS sample buffer and run on 10% SDS-PAGE gels. Western blots were probed with mouse anti-FLAG (M2) or mouse anti-Myc (9E10) antibodies (Sigma-Aldrich).

RESULTS

Mutations in the *C. elegans* neogenin homolog *unc-40* cause phenotypes resembling those of Sma/Mab pathway mutants

The *C. elegans* BMP-like Sma/Mab pathway regulates body size and male tail patterning (Savage-Dunn, 2005). Mutations in this pathway can also suppress the mesodermal M lineage phenotypes of *sma-9(0)* mutants (Foehr et al., 2006; Tian et al., 2010). Specifically, the two coelomocytes (CCs) derived from the dorsal M lineage (Fig. 1C) are missing in *sma-9(0)* mutants due to a dorsal-to-ventral fate transformation in the M lineage (Fig. 1A,D). These two CCs can be restored in double mutants between *sma-9(0)* and mutations in Sma/Mab pathway members (Fig. 1B,C). In a large-scale screen for mutations that could suppress the loss-of-M-derived CCs phenotype of *sma-9(cc604)* mutants (the mutagenesis screen will be described in a separate manuscript), we identified a recessive mutation *jj59* that exhibited a penetrance of 73.3% (n=195) of suppression of the *sma-9(cc604)* M lineage phenotype (SOSMLP) (Table 1). Genetic mapping, complementation test and sequencing showed that *jj59* is a nonsense mutation (Q628Stop, CAA to TAA) in the sole *C. elegans* neogenin and DCC homolog *unc-40* (Table 1, Table 3A). A canonical *unc-40* null allele, *e1430* (Hedgecock et al., 1990), also suppressed the M lineage phenotype of *sma-9(cc604)* mutants (88.7%, n=150, Table 1). Both *unc-40(jj59)* and *unc-40(e1430)* mutants also have a significantly smaller body size than wild-type worms at the same developmental stage (Table 1). Thus, *unc-40* mutants exhibit phenotypes of Sma/Mab pathway mutants.

Mutations in the *C. elegans* netrin ortholog *unc-6* and the netrin receptor gene *unc-5* do not exhibit Sma/Mab pathway mutant phenotypes

UNC-40 has been well studied as a DCC ortholog that functions as a netrin receptor in both UNC-5-dependent and UNC-5-independent pathways to mediate axonal and cellular movement guidance (Hedgecock et al., 1990; Kennedy et al., 1994; Chan et al., 1996;

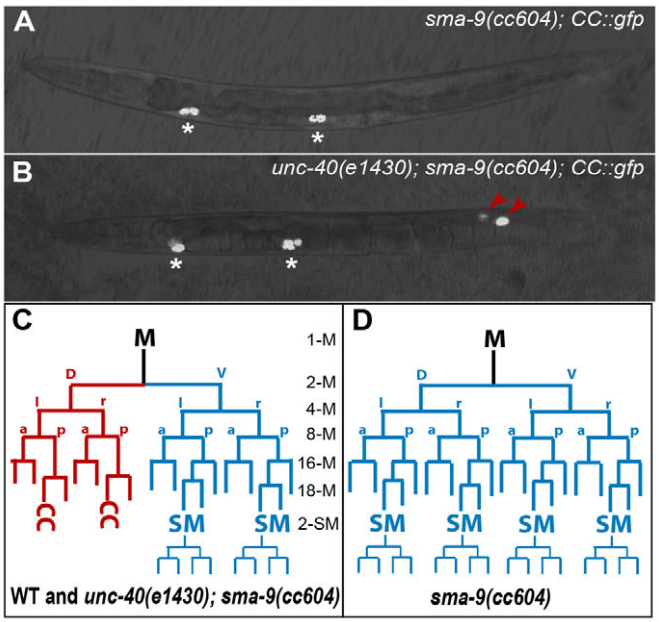

Fig. 1. *unc-40*, but not *unc-5* or *unc-6*, mutants exhibit body size and mesoderm defects. (**A**,**B**) Images illustrating the mesoderm phenotype (lateral views with anterior to the left and dorsal up). *CC::gfp* labels all the coelomocytes (CCs), including embryonically derived CCs (asterisks) and M-derived CCs (red arrowheads). (**C**,**D**) Schematic representation of the M lineage. *sma-9(cc604)* mutants (A,D) exhibit a dorsal-to-ventral fate transformation in the M lineage, leading to the lack of M-derived CCs compared with wild type (C) or *unc-40(e1430); sma-9(cc604)* double mutants (B,C). SM, sex myoblast; a, anterior; d, dorsal; l, left; p, posterior; r, right; v, ventral.

Colón-Ramos et al., 2007; Teichmann and Shen, 2011). We investigated whether UNC-6/netrin and UNC-5 play a role in modulating Sma/Mab signaling by examining the null mutants of *unc-6* and *unc-5* for Sma/Mab pathway mutant phenotypes, including the suppression of the *sma-9(0)* M lineage phenotype (SOSMLP) and the small body size phenotype. Unlike *unc-40* null mutants, null mutants in *unc-6(ev400)* and *unc-5(e53)* (Hedgecock et al., 1990; Wadsworth et al., 1996) did not exhibit any Sma/Mab pathway mutant phenotypes (Table 1). Interestingly, Hedgecock and colleagues noted a 'DUMPY' phenotype for *unc-40*, but not *unc-5* and *unc-6*, alleles (Hedgecock et al., 1990). Thus, UNC-40 appears to play a role in Sma/Mab signaling independent of UNC-6 and UNC-5.

UNC-40 functions at the ligand-receptor level to positively modulate Sma/Mab signaling

The shared phenotypes between *unc-40* mutants and Sma/Mab pathway mutants suggest that *unc-40* might function in the Sma/Mab pathway. This pathway includes the ligand DBL-1 (Morita et al., 1999; Suzuki et al., 1999), the type I receptor SMA-6 (Krishna et al., 1999), the type II receptor DAF-4 (Estevez et al., 1993) and R-Smads SMA-2 and SMA-3, as well as co-Smad SMA-4 (Savage et al., 1996). We carried out two sets of experiments to test this hypothesis. First, we examined the activity of the RAD-SMAD reporter in *unc-40(e1430)* null mutants. The RAD-SMAD reporter activity positively correlates with Sma/Mab pathway activity at the transcriptional level (Tian et al., 2010). The RAD-SMAD reporter activity was decreased in *unc-40(e1430)* mutants compared with wild-type animals (Fig. 2C). As controls, the RAD-SMAD reporter activity is increased in *lon-2(e678)*, an allele with hyperactive Sma/Mab signaling (Gumienny et al., 2007), and decreased in the ligand null *dbl-1(wk70)* (Morita et al., 1999; Suzuki et al., 1999) and in an RGM protein null *drag-1(jj4)*. These results suggest that UNC-40 functions as a positive modulator of the Sma/Mab pathway.

Second, we carried out genetic epistasis experiments by generating double mutants between *unc-40(e1430)* and null mutations in various Sma/Mab pathway components (Fig. 2A) and measuring their body sizes. *unc-40(e1430); sma-3(jj3)* and *unc-40(e1430); dbl-1(wk70)* double mutants were as small as *sma-3(jj3)* and *dbl-1(wk70)* single mutants, respectively (Fig. 2B), suggesting that *unc-40* is likely to function within the Sma/Mab pathway in regulating body size. To further determine where in the Sma/Mab pathway *unc-40* might function, we generated the following double mutants: *unc-40(e1430); lon-1(jj67)* and *unc-40(e1430); lon-2(e678)*. *jj67* is an apparent null mutation in *lon-1*, a gene negatively regulated by the Sma/Mab pathway (Maduzia et al., 2002; Morita et al., 2002) (our unpublished results). *e678* is a null mutation in *lon-2*, which encodes a member of the glypican family of heparan sulfate proteoglycans and acts as a negative regulator of Sma/Mab signaling, presumably by sequestering the DBL-1 ligand (Gumienny et al., 2007). We found that *unc-40(e1430); lon-1(jj67)* mutants were as long as *lon-1(jj67)* mutants (Fig. 2B), again suggesting that *unc-40* functions within the Sma/Mab pathway, upstream of *lon-1*, to regulate body size. Interestingly, *unc-40(e1430); lon-2(e678)* mutants showed an intermediate body size between *unc-40(e1430)* mutants and *lon-2(e678)* mutants. These results suggest that *unc-40* is likely to function in parallel to *lon-2*, a negative regulator of the Sma/Mab pathway that acts at the ligand-receptor level. Taken together, our results indicate that *unc-40* is likely to function at the ligand-receptor level to positively modulate Sma/Mab signaling.

UNC-40 is expressed and functions in the Sma/Mab signal-receiving cells

We next examined the expression pattern of an integrated UNC-40::GFP transgene that is functional in mediating axon guidance (Chan et al., 1996). This transgene rescued the small body size and SOSMLP phenotypes of *unc-40(e1430)* mutants (Table 3B, the

Table 1. Summary of body size and mesodermal phenotypes in *unc-40*, *unc-5* and *unc-6* null mutants

Genotype	Molecular lesions	Relative body length	SOSMLP (%)
WT		1.16±0.06*** (*n*=27)	N.A.
unc-40(e1430)	R157STOP (null)	1.00±0.04 (*n*=50)	88.7 (*n*=150)
unc-40(jj59)	Q628STOP	0.99±0.06 (*n*=46)	73.3 (*n*=195)
unc-5(e53)	W283STOP (null)	1.14±0.05*** (*n*=39)	1.7 (*n*=59)
unc-6(ev400)	Q78STOP (null)	1.14±0.06*** (*n*=20)	0.5 (*n*=221)

Body length data shown here and in subsequent figures and tables were normalized over that of *unc-40(e1430)* mutants. Data are mean ± s.d. ***P<0.0001, *unc-40(e1430)* versus other mutants (Student's *t*-test).
SOSMLP, suppression of the *sma-9* M lineage phenotype.
N.A., not applicable.

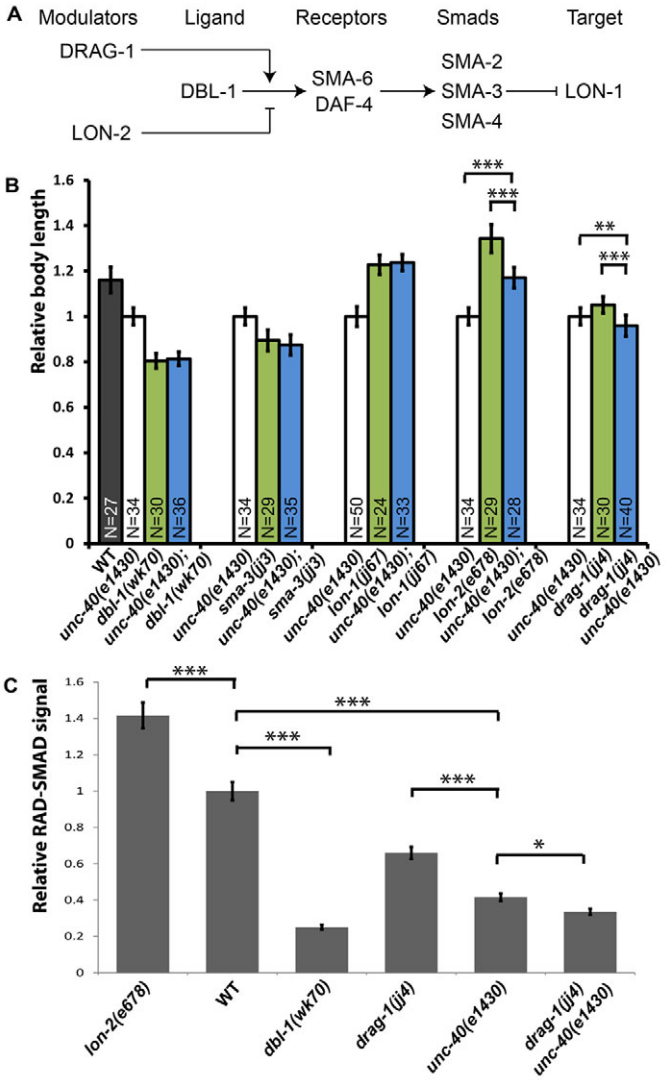

Fig. 2. *unc-40* functions at the ligand-receptor level to positively regulate Sma/Mab signaling. (**A**) The Sma/Mab pathway. (**B**) Relative body lengths of stage-matched wild-type (WT) and various mutant worms measured at the Christmas tree stage of vulval development (see Materials and methods). (**C**) Quantification of hypodermal RAD-SMAD GFP signals in various mutants compared with wild-type animals (set to 1). (B,C) ***P<0.0001, **P<0.001, *P<0.05 (Student's t-test). Error bars represent s.d.

UNC-40 wild-type transgene). Sma/Mab pathway receptors and Smads are known to be expressed and to function in the hypodermal cells to regulate body size and in the M lineage to regulate M lineage development (Yoshida et al., 2001; Wang et al., 2002; Foehr et al., 2006). We found that, in addition to the previously reported neuronal and muscle cell expression (Chan et al., 1996; Alexander et al., 2009), the functional UNC-40::GFP transgene is expressed in both hypodermal cells (Fig. 3A-C) and M lineage cells (Fig. 3D-O). Thus, *unc-40* is expressed in the signal-receiving cells of the Sma/Mab pathway.

To determine whether UNC-40 functions in the signal-receiving cells of the Sma/Mab pathway, we forced the expression of the *unc-40* cDNA in hypodermal cells using both the *elt-3* and *rol-6* promoters (Kramer and Johnson, 1993; Gilleard et al., 1999) and in the M lineage using the *hlh-8* promoter (Harfe et al., 1998). Forced expression of *unc-40* in hypodermal cells rescued the small body size phenotype (Table 2), and forced expression of *unc-40* in the M lineage rescued the SOSMLP phenotype (SOSMLP down to 4.1%; n=49), of *unc-40(e1430)* mutants. However, forced expression of *unc-40* in body-wall muscles using the *myo-3* promoter (Fire et al., 1998) failed to rescue the small body size phenotype (Table 2). As a positive control, expression of *unc-40* cDNA under the control of its own promoter was able to rescue the small body size phenotype of *unc-40(e1430)* mutants (Table 2). Similarly, expression of *unc-40* under its own promoter or under the pan-neuronal promoter *unc-119* (Maduro and Pilgrim, 1995), but not under hypodermal- or muscle-specific promoters, rescued the axonal migration defects of *unc-40(e1430)* mutants (Table 2), consistent with the fact that UNC-40 functions as a netrin receptor in neuronal cells to regulate their axonal path finding (Chan et al., 1996). Taken together, our findings are consistent with UNC-40 functioning in the signal-receiving cells to modulate Sma/Mab signaling. Interestingly, forced expression of *unc-40* in all neuronal cells using the *unc-119* promoter partially rescued the small body size phenotype of *unc-40(e1430)* mutants (Table 2). This partial rescue could reflect a role of UNC-40 in the signal-producing cells, as the DBL-1 ligand is produced in the ventral nerve cord cells (Morita et al., 1999; Suzuki et al., 1999). Alternatively, it could be an indirect result of the less uncoordinated phenotype of the transgenic animals.

The extracellular domain of UNC-40 is sufficient to modulate Sma/Mab signaling

unc-40 has been studied extensively in terms of its roles in axonal and cell migration (Culotti and Merz, 1998; Blelloch et al., 1999; Quinn and Wadsworth, 2008; Alexander et al., 2009). Thus, multiple *unc-40* alleles exist. To understand which domain of UNC-40 is required for its role in Sma/Mab signaling, we examined multiple *unc-40* alleles for body size and SOSMLP phenotypes. Four nonsense mutations, *e1430* (R157STOP), *ev457* (W460STOP), *e271* [R827STOP (Hedgecock et al., 1990; Chan et al., 1996)] and *jj59* (Q628STOP), which truncate the extracellular domain of UNC-40, all exhibited highly penetrant small body size and SOSMLP phenotypes (Table 3A). However, *ev495* (Q1075STOP; Joe Culotti, personal communication) and *tr115* [W1107STOP (Alexander et al., 2009)], which truncate the UNC-40 protein right before and right after the transmembrane (TM) domain, respectively (Table 3A), failed to suppress the *sma-9* M lineage phenotype, and the body sizes of *ev495* and *tr115* mutants were significantly longer than that of *e1430* mutants and not statistically different from that of wild-type worms (Table 3A). This is in stark contrast to the axon guidance and cell migration defects shared by all these mutant alleles (Table 3A).

The above findings raised the possibility that the extracellular domain (EXD) of UNC-40 is sufficient to mediate Sma/Mab signaling. To test this hypothesis and to rule out the possibility that potential full-length UNC-40 proteins are present in *ev495* and *tr115* mutants due to alternative splicing, thus bypassing the nonsense mutations, we generated a transgene containing UNC-40 EXD only and introduced it into the null *unc-40(e1430)* background. Whereas the full-length UNC-40 transgene rescued the body size, SOSMLP, and axon and cell migration defects of *unc-40(e1430)* mutants, the transgene containing UNC-40 EXD only rescued the body size and SOSMLP phenotypes, but not the axon and cell migration defects of *unc-40(e1430)* mutants (Table 3B). These results demonstrate that, although the intracellular domain (ICD) of UNC-40 is essential for its role in axon guidance and cell migration, this domain is not required in mediating Sma/Mab signaling; instead, UNC-40 EXD is sufficient

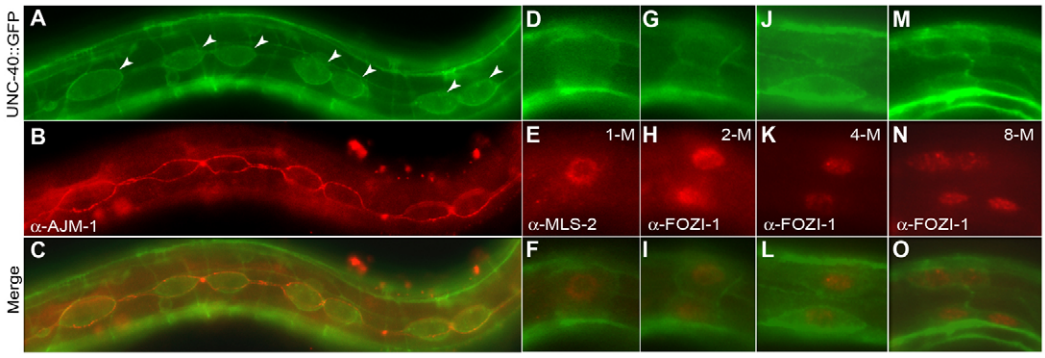

Fig. 3. UNC-40 is expressed and functions in the Sma/Mab signal-receiving cells. (**A-C**) UNC-40::GFP (green) is localized to the cellular membrane of the hypodermal seam cells (arrowheads in A), as indicated by anti-AJM-1 antibody staining (red, B). (**D-O**) UNC-40::GFP (green, D,G,J,M) is localized to the surface of M lineage cells marked by anti-MLS-2 and anti-FOZI-1 antibody staining (E,H,K,N) from the 1-M to the 8-M stage. Only one focal plane is shown for the 4-M (J-L) and 8-M (M-O) stage worms.

to function in Sma/Mab signaling. These results also suggest that the function of UNC-40 in mediating Sma/Mab signaling is independent from its function in axon guidance and cell migration.

The sixth fibronectin type III motif (FN6) of UNC-40 is essential for its role in Sma/Mab signaling

Our analyses of the *unc-40* mutant alleles also suggested that the fifth and sixth fibronectin type III (FNIII) motifs are important for UNC-40 function in Sma/Mab signaling (compare the SOSMLP phenotypes of *e271* and *ev495* in Table 3A). To test this hypothesis and to rule out the possibility that the phenotypes of these two alleles were due to the absence of mutant UNC-40 proteins as a result of nonsense-mediated decay of the mutant mRNAs, we generated *unc-40* transgenes with the fifth or the sixth or both of these FNIII motifs deleted (ΔFN5, ΔFN6 or ΔFN5,6, respectively). Whereas ΔFN5 rescued both the small body size and the SOSMLP phenotypes of the null *unc-40(e1430)* mutants, ΔFN6 and ΔFN5,6 failed to rescue these two phenotypes (Table 3B). All three deletion constructs completely rescued the axon guidance and cell migration phenotypes of *unc-40(e1430)* mutants. These results demonstrate that FN6 is absolutely required for the function of UNC-40 in Sma/Mab signaling. Moreover, both FN5 and FN6 are dispensable for the role of UNC-40 in axon guidance and cell migration.

The FN6 motif is required for UNC-40 and DRAG-1 interaction and is essential for UNC-40 function in Sma/Mab signaling

Neogenin, but not DCC, has been shown to directly bind to RGMc through the FN6 motif (Yang et al., 2008). Both neogenin and RGMc have been implicated in BMP signaling (Corradini et al., 2009; Severyn et al., 2009). We have previously shown that the *C. elegans* RGM protein DRAG-1 is a positive modulator of Sma/Mab signaling (Tian et al., 2010). The finding that the FN6 motif is crucial for UNC-40 function in Sma/Mab signaling led us to hypothesize that UNC-40 might function together with the *C. elegans* RGM protein DRAG-1 through the FN6 motif. To test this, we transiently expressed the FN5,6 fragment of UNC-40 and the mature portion of DRAG-1 lacking the N- and C-terminal signal sequences in HEK293T cells and performed co-immunoprecipitation (co-IP) assays. We found that FLAG-tagged DRAG-1 could co-immunoprecipitate with Myc-tagged FN5,6 fragment of UNC-40 (Fig. 4C).

To identify the specific sequences in FN6 that are required for the UNC-40–DRAG-1 interaction, we took advantage of the crystal structure of the FN5,6 motifs of human neogenin (Yang et al., 2011). The amino acids involved in neogenin-RGM interaction are predicted to be exposed to the surface of FN6 and to be divergent between human neogenin and DCC (Yang et al., 2011). We also expected them to be conserved among the UNC-40 proteins in different *Caenorhabditis* species. Based on these criteria, we picked three clusters of amino acids located in the C-C′ loop, C′ strand or the E-F loop based on the crystal structure of the human neogenin FN6 domain (Yang et al., 2011) (Fig. 4A,B). We tested the importance of each of the three regions by mutating the residues in each region to their corresponding sequences in the human DCC protein. We then examined the consequences of each mutation on the interaction between UNC-40 and DRAG-1 using the co-IP assay and on the *in vivo* function of UNC-40 using the transgene rescue assay described above. Mutations in the E-F loop, but not those in

Table 2. Rescue of axon guidance defects (Unc, Egl and AVM migration) and Sma/Mab signaling defects (body size) of *unc-40(e1430)* worms by tissue-specific expression of *unc-40* cDNA

unc-40 alleles	Transgenes	Unc	Egl (%)	AVM migration defect (%)	Relative body length
WT	None	1 (*n*>100)	0 (*n*>100)	0 (*n*>100)	1.16±0.06*** (*n*=27)
unc-40(e1430)	None	3.2 (*n*=54)	33.3 (*n*=54)	25.4 (*n*=51)	1.00±0.04 (*n*=50)
unc-40(e1430)	*unc-40p::unc-40 cDNA*	1.6 (*n*=50)	16 (*n*=50)	14.8 (*n*=108)	1.11±0.04*** (*n*=73)
unc-40(e1430)	*elt-3p::unc-40 cDNA*	2.7 (*n*=37)	21.6 (*n*=37)	28.0 (*n*=118)	1.09±0.05*** (*n*=62)
unc-40(e1430)	*rol-6p::unc-40 cDNA*	2.8 (*n*=90)	26.7 (*n*=90)	27.9 (*n*=106)	1.10±0.04*** (*n*=60)
unc-40(e1430)	*unc-119p::unc-40 cDNA*	1.9 (*n*=58)	15.9 (*n*=63)	10.2 (*n*=117)	1.03±0.04*** (*n*=70)
unc-40(e1430)	*myo-3p::unc-40 cDNA*	2.5 (*n*=103)	25.4 (*n*=114)	22.9 (*n*=109)	1.00±0.05 (*n*=80)

For axon guidance defects, see supplementary material Fig. S1. Body length was normalized over that of *unc-40(e1430)* mutants. For all the measurements on transgenic worms in Tables 2-5, data from two transgenic lines were pooled and averaged. ***P<0.0001.
Unc, uncoordinated movement; Egl, egg-laying defective.

Table 3. The UNC-40 EXD is sufficient to function in Sma/Mab signaling and requires the FN6 motif

(A) Axon guidance defects (Unc, Egl and AVM migration) and Sma/Mab signaling defects (body size and SOSMLP) in different *unc-40* mutant backgrounds

Genotype	Endogenous UNC-40	Unc	Egl (%)	AVM migration defect (%)	Relative body length	SOSMLP (%)
WT		1 (*n*>100)	0 (*n*>100)	0 (*n*>100)	1.16±0.06*** (*n*=27)	N.A.
unc-40(e1430) R157STOP		3.0 (*n*=54)	33.3 (*n*=54)	25.4 (*n*=51)	1.00±0.04 (*n*=50)	88.7 (*n*=150)
unc-40(ev457) W460STOP		N.D.	N.D.	N.D.	N.D.	72.8 (*n*=158)
unc-40(jj59) Q628STOP		N.D.	N.D.	N.D.	0.99±0.06 (*n*=46)	73.3 (*n*=195)
unc-40(e271) R827STOP		N.D.	N.D.	N.D.	N.D.	73.1 (*n*=188)
unc-40(ev495) Q1075STOP		3.2 (*n*=50)	34 (*n*=50)	27.9 (*n*=61)	1.14±0.05*** (*n*=28)	2.7 (*n*=221)
unc-40(tr115) W1107STOP		3.0 (*n*=50)	32 (*n*=50)	42.3 (*n*=52)	1.13±0.04*** (*n*=28)	0 (*n*=166)

(B) Axon guidance defects and Sma/Mab signaling defects in *unc-40(e1430)* mutants expressing different *unc-40* transgenes

Genotype	Unc	Egl (%)	AVM migration defect (%)	Relative body length	SOSMLP (%)
WT	1 (*n*>100)	0 (*n*>100)	0 (*n*>100)	1.16±0.06*** (*n*=27)	N.A.
unc-40(e1430)	3.0 (*n*=54)	33.3 (*n*=54)	25.4 (*n*=51)	1.00±0.04 (*n*=50)	88.7 (*n*=150)
UNC-40 WT in *unc-40(e1430)* 	2.3 (*n*=101)	25.7 (*n*=101)	14.5 (*n*=117)	1.12±0.05*** (*n*=51)	1.8 (*n*=57)
UNC-40 ΔFN5 in *unc-40(e1430)* 	2.2 (*n*=107)	25.0 (*n*=124)	21.6 (*n*=111)	1.13±0.05*** (*n*=55)	3.3 (*n*=61)
UNC-40 ΔFN6 in *unc-40(e1430)* 	2.2 (*n*=100)	22.3 (*n*=130)	11.5 (*n*=122)	0.98±0.06 (*n*=53)	93.6 (*n*=47)
UNC-40 ΔFN5,6 in *unc-40(e1430)* 	2.2 (*n*=76)	28.9 (*n*=76)	13.9 (*n*=108)	0.98±0.06 (*n*=56)	96.9 (*n*=64)
UNC-40 EXD in *unc-40(e1430)* 	3.3 (*n*=123)	43.1 (*n*=144)	31.7 (*n*=104)	1.08±0.04*** (*n*=50)	8.3 (*n*=48)
Mouse Neo1 in *unc-40(e1430)* 	N.D.	N.D.	N.D.	1.05±0.03*** (*n*=21)	75.9 (*n*=323)
Mouse DCC in *unc-40(e1430)* 	N.D.	N.D.	N.D.	1.00±0.05 (*n*=66)	97.2 (*n*=109)

***P<0.0001. Purple squares, Immunoglobin domains (IGs); blue ovals, fibronectin type III domains (FNs); double black lines, transmembrane domain (TM); white ovals, P1, P2, P3 motifs; red cross, domain(s) deleted. The mouse Neo1 (shaded purple) and DCC (shaded yellow) constructs are described in Materials and methods and supplementary material Table S1.
N.A., not applicable; N.D., not determined.

the C-C′ loop and C′ strand, abolished both the interaction between UNC-40 and DRAG-1 (Fig. 4C) and the function of UNC-40 *in vivo* (Table 4). All three mutant *unc-40* transgenes could still function in mediating axon guidance (Table 4), again confirming that axon guidance and Sma/Mab signaling are two independent functions mediated by different regions of the UNC-40 protein. These results also indicated that the interaction between UNC-40 and DRAG-1 is crucial for UNC-40 function in Sma/Mab signaling *in vivo*.

The function of DRAG-1 in modulating Sma/Mab signaling requires DRAG-1–UNC-40 interaction

We next asked whether disrupting the interaction between DRAG-1 and UNC-40 also compromises the function of DRAG-1 in modulating Sma/Mab signaling. Mutations in RGMc (HFE2) cause juvenile hemochromatosis (JH) (Papanikolaou et al., 2004). Previous studies on the JH-causing mutations in RGMc showed that the G320V mutation disrupted the interaction between RGMc and neogenin (Kuns-Hashimoto et al., 2008). Glycine G320 is absolutely conserved and corresponds to G272 in DRAG-1 (supplementary material Fig. S2). We made a corresponding G272V mutation in DRAG-1 and tested its effect on DRAG-1–UNC-40 interaction via the co-IP assay and on DRAG-1 function *in vivo* using the transgenic rescue assay. DRAG-1^{G272V} exhibited a greatly reduced ability to interact with the FN5,6 fragment of UNC-40 (Fig. 5A,B), and it failed to function *in vivo* (Table 5), even though it is expressed at similar levels to a wild-type *drag-1* transgene (Fig. 5C). These results indicated that, as for UNC-40, DRAG-1–UNC-40 interaction is crucial for DRAG-1 function in Sma/Mab signaling.

Taken together, our findings suggested that DRAG-1 and UNC-40 are likely to function together to promote Sma/Mab signaling. Consistent with this, genetic epistasis analysis between *unc-40* and *drag-1* showed that, regarding body size regulation, DRAG-1 and UNC-40 have largely overlapping functions. *drag-1(jj4) unc-40(e1430)* double mutants are only slightly smaller than either *drag-1(jj4)* or *unc-40(e1430)* single mutants (Fig. 2B), which does not appear to be a result of either additive or synergistic effects of the two mutations.

DRAG-1 interacts with both the ligand and receptors of the Sma/Mab pathway

RGM proteins are known to bind the ligand as well as both the type I and type II receptors of the BMP pathway (Babitt et al.,

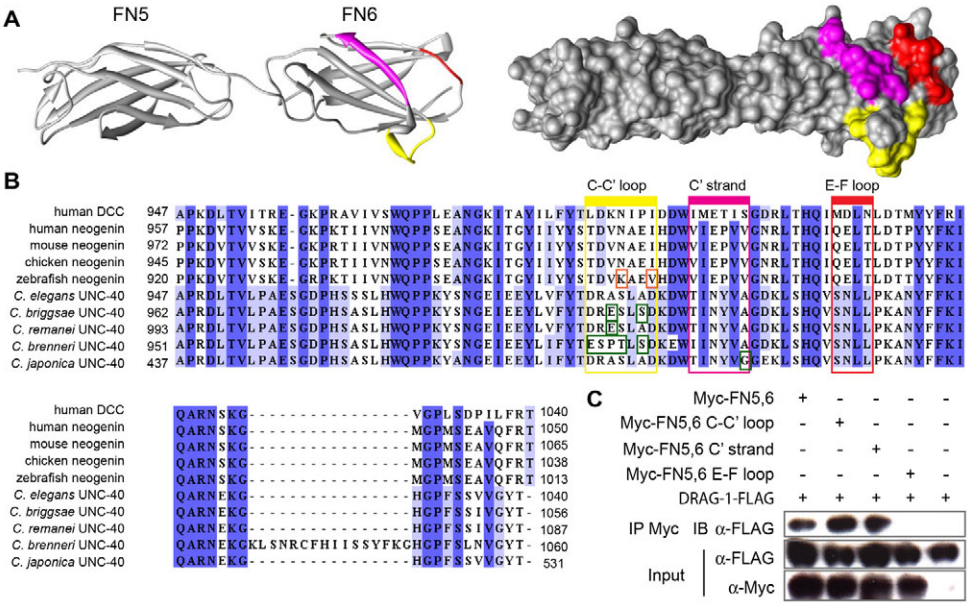

Fig. 4. The E-F loop in FN6 of UNC-40 is crucial for interaction with DRAG-1 and for UNC-40 function in Sma/Mab signaling. (**A**) Crystal structure of human neogenin FN5 and FN6 domains [PDB ID: 3P4L (Yang et al., 2011)] in ribbon (left) and surface view (right) as presented by Chimera software (Pettersen et al., 2004), with the C-C′ loop (yellow), C′ strand (purple) and E-F loop (red) highlighted. (**B**) Alignment of the FN6 domains of *C. elegans* UNC-40 and its vertebrate and nematode homologs. Conserved residues are in blue. Small red boxes highlight the divergent residues between human neogenin and other vertebrate neogenins. Small green boxes highlight the divergent residues between *C. elegans* UNC-40 and UNC-40 from other nematode species. (**C**) Co-immunoprecipitation (co-IP) between DRAG-1-FLAG and Myc-tagged FN5,6, or Myc-tagged FN5,6 with the C-C′ loop, C′ strand or E-F loop mutated.

2005; Samad et al., 2005; Babitt et al., 2006). Thus, we tested whether DRAG-1 can bind to the ligand and receptors of the Sma/Mab pathway. For co-IP assays we expressed all the factors in HEK293T cells. As a control, the ligand DBL-1 interacts with the type I receptor SMA-6 but not the type II receptor DAF-4 (Fig. 5E), consistent with previous findings that BMP2 and BMP4, the closest homologs of DBL-1, have a higher affinity to type I receptors than to type II receptors (Allendorph et al., 2006). Like its vertebrate homologs, DRAG-1 also interacts with the ligand DBL-1, the type I receptor SMA-6, and the type II receptor DAF-4 (Fig. 5D,E).

The interaction between DRAG-1 and DBL-1 also appears to be important for DRAG-1 function *in vivo*. A G68V mutation in DRAG-1, which corresponds to G99V in human RGMc, which disrupts RGMc-BMP interaction (Kuns-Hashimoto et al., 2008), significantly affected the function of DRAG-1, as the *drag-1*^{G68V} transgene only partially rescued the small body size and SOSMLP phenotypes of *drag-1(jj4)* mutants (Fig. 5A, Table 5). A *drag-1* transgene containing a D127E mutation, *drag-1*^{D127E}, rescued the small body size and SOSMLP phenotypes of *drag-1(jj4)* mutants, just like the wild-type *drag-1* transgene (Fig. 5A, Table 5). D127E in DRAG-1 corresponds to D172E in human RGMc, which disrupts the intramolecular cleavage of RGMc (Kuns-Hashimoto et al., 2008). Thus, DRAG-1 might not undergo autocleavage in *C. elegans*, or this cleavage is not crucial for DRAG-1 function.

Evolutionarily conserved functions of RGM/DRAG-1 and neogenin/UNC-40 in modulating BMP signaling

The similarities in function between DRAG-1 and vertebrate RGMs and between UNC-40 and neogenin prompted us to examine whether vertebrate neogenin and RGMs can substitute for the functions of DRAG-1 and UNC-40, respectively, in *C. elegans*. Directly expressing the mouse *Rgmb* cDNA under the control of the *drag-1* promoter failed to rescue the *drag-1(jj4)* mutant phenotypes (data not shown). However, hybrid transgenes with the DRAG-1 mature protein sequence replaced by those of mouse RGMb (mouse *Rgmb-drag-1*) or human RGMc (human *Rgmc-drag-1)*, when driven by the *drag-1* promoter, could partially rescue the small body

Table 4. Rescue of axon guidance defects (Unc, Egl and AVM migration) and Sma/Mab signaling defects (body size and SOSMLP) of *unc-40(e1430)* mutants by various *unc-40* transgenes

unc-40 alleles	Transgenes	Unc	Egl (%)	AVM migration defect (%)	Relative body length	SOSMLP (%)
WT	None	1 (*n*>100)	0 (*n*>100)	0 (*n*>100)	1.16±0.06*** (*n*=27)	N.A.
unc-40(e1430)	None	3.0 (*n*=54)	33.3 (*n*=54)	25.4 (*n*=51)	1.00±0.04 (*n*=50)	88.7 (*n*=150)
unc-40(e1430)	*unc-40* WT	2.3 (*n*=101)	25.7 (*n*=101)	14.5 (*n*=117)	1.12±0.05*** (*n*=51)	1.8 (*n*=57)
unc-40(e1430)	*unc-40* C-C′	1.2 (*n*=111)	22.1 (*n*=104)	18.8 (*n*=106)	1.13±0.05*** (*n*=51)	0 (*n*=108)
unc-40(e1430)	*unc-40* C′	1.3 (*n*=114)	18.3 (*n*=104)	15.7 (*n*=108)	1.11±0.06*** (*n*=54)	3.9 (*n*=158)
unc-40(e1430)	*unc-40* E-F	1.3 (*n*=103)	25.2 (*n*=103)	16.7 (*n*=114)	1.01±0.05 (*n*=43)	81.8 (*n*=143)

***P<0.0001.

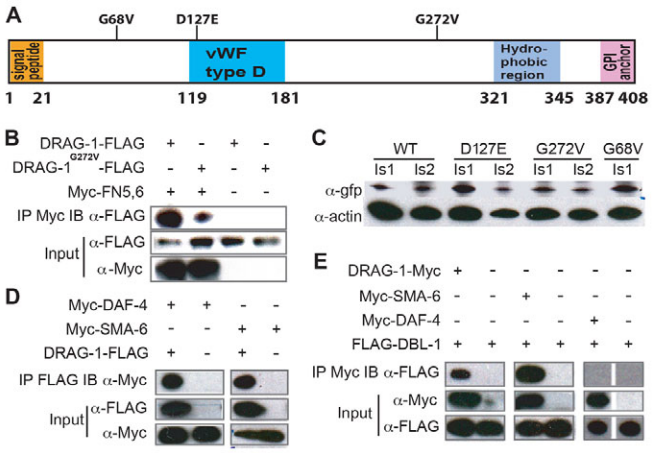

Fig. 5. DRAG-1 mediation of Sma/Mab signaling is most likely dependent on its physical association with UNC-40. (**A**) The DRAG-1 protein, illustrating the point mutations tested. See supplementary material Fig. S2 for details. (**B**) co-IP between DRAG-1 or DRAG-1^{G272V} and UNC-40 FN5,6. (**C**) Western blot on worm lysates from Mos-mediated single-copy insertion lines carrying the wild-type or mutant *drag-1::gfp* transgenes listed in Table 5. DRAG-1::GFP proteins are recognized by anti-GFP. Actin is used as a loading control. (**D**,**E**) Co-IP between DRAG-1 and SMA-6 (D), DAF-4 (D) and DBL-1 (E), and between DBL-1 and SMA-6 or DAF-4 (E). The separated blots on the far right in E are non-abutting lanes cut from the same film.

size and SOSMLP phenotypes of *drag-1(jj4)* mutants (Table 5). Similarly, a hybrid transgene with the signal sequence of mouse neogenin (Neo1) replaced by that of UNC-40 could partially rescue the small body size and SOSMLP phenotypes of *unc-40(e1430)* mutants (Table 3B). By contrast, a similar hybrid transgene containing mouse DCC failed to rescue the small body size and SOSMLP phenotypes of *unc-40(e1430)* mutants (Table 3B). These results suggest that DRAG-1 and UNC-40 and their corresponding vertebrate counterparts share evolutionarily conserved functions in modulating BMP signaling.

Mouse neogenin does not require its intracellular domain to promote BMP signaling

We have described that the EXD of UNC-40 is sufficient to mediate Sma/Mab signaling in *C. elegans*. Because of the functional conservation between UNC-40 and mouse neogenin, we next tested whether mouse neogenin requires its ICD to promote BMP signaling using two independent assays. First, we expressed full-length neogenin (Neo) or neogenin with the ICD deleted (NeoΔICD) in HEK293 cells and determined their effect on BMP2-stimulated phosphorylation of Smad1/5/8. Both Neo and NeoΔICD enhanced BMP2-stimulated phosphorylation of Smad1/5/8 to a similar extent (Fig. 6A,B). Second, we transfected Neo and NeoΔICD into primary fibroblast cells derived from neogenin hypomorphic mutant mice (Zhou et al., 2010) and determined their ability to rescue the defective expression of a BMP signaling reporter (9XSBE-Luc) upon BMP2 stimulation. Both Neo and NeoΔICD restored the BMP2-stimulated expression of the BMP signaling reporter to a similar extent (Fig. 6C). These results demonstrate that, like *C. elegans* UNC-40, the ICD of mouse neogenin is not required for proper BMP signaling.

DISCUSSION

UNC-40/neogenin positively modulates BMP signaling

As a close homolog of DCC, neogenin was initially recognized as an axon guidance receptor that is required for axon and cell migration (Cole et al., 2007; Wilson and Key, 2007; Yamashita et al., 2007). Recent reports suggest that neogenin is also involved in modulating BMP signaling, but how it does so has been controversial (Tian and Liu, 2013). On the one hand, neogenin positively potentiates BMP signaling to regulate the expression of hepcidin for body iron metabolism and endochondral ossification in mice (Lee et al., 2010; Zhou et al., 2010) or human liver cells (Zhang et al., 2009). On the other hand, neogenin negatively modulates BMP2-induced osteoblastic differentiation of C2C12 cells (Hagihara et al., 2011). Neogenin also increases the secretion of soluble RGMc, which may cause downregulation of BMP signaling (Zhang et al., 2005; Zhang et al., 2007).

Our findings clearly demonstrate that the sole DCC/neogenin homolog UNC-40 is a positive modulator of the BMP-like Sma/Mab pathway in *C. elegans*: (1) *unc-40(0)* mutants share similar body size and SOSMLP phenotypes with those of Sma/Mab pathway loss-of-function mutants; (2) *unc-40(0)* mutants exhibit reduced activity of the Sma/Mab reporter, RAD-SMAD; and (3) *unc-40* acts in the Sma/Mab pathway to regulate body size, as indicated by the genetic epistasis analysis. We further showed that UNC-40 functions at the ligand-receptor level in the signal-receiving cells to modulate Sma/Mab signaling. Because mouse neogenin can partially rescue the Sma/Mab pathway phenotypes of *unc-40(0)* mutants, we suggest that, like its function in axon guidance and cell migration, the function of UNC-40 in modulating BMP signaling is also evolutionarily conserved.

UNC-40 independently mediates BMP signaling and netrin signaling

DCC is well established as a receptor for netrin in axon guidance and migration (Kennedy et al., 1994; Colavita and Culotti, 1998; Hong et al., 1999; Qin et al., 2007). Unlike DCC, which does not bind RGM proteins, neogenin can bind to both netrin and RGM

Table 5. Body size and SOSMLP phenotypes of *drag-1(jj4)* mutants expressing various transgenes

Genotype	Relative body length	SOSMLP (%)
WT	1.18±0.05*** (*n*=48)	N.A.
drag-1(jj4)	1.00±0.05 (*n*=50)	98.5 (*n*=201)
drag-1(jj4) + *drag-1* cDNA	1.10±0.06*** (*n*=25)	82.1 (*n*=106)
drag-1(jj4) + mouse *Rgmb* cDNA	1.04±0.04*** (*n*=34)	85.4 (*n*=82)
drag-1(jj4) + human *Rgmc* cDNA	1.03±0.04*** (*n*=72)	76.6 (*n*=143)
drag-1(jj4) + Mos-SCI *drag-1::gfp*	1.17±0.04*** (*n*=96)	1.2 (*n*=498)
drag-1(jj4) + Mos-SCI *drag-1(G68V)::gfp*	1.02±0.04* (*n*=47)	79.3 (*n*=554)
drag-1(jj4) + Mos-SCI *drag-1(D127E)::gfp*	1.04±0.04*** (*n*=76)	0.8 (*n*=515)
drag-1(jj4) + Mos-SCI *drag-1(G272V)::gfp*	1.01±0.04 (*n*=98)	94.9 (*n*=414)

Body length was normalized to that of *drag-1(jj4)* mutants. Data are mean ± s.d. ***P<0.0001, *P<0.05, *drag-1(jj4)* versus worms of different genotypes (Student's *t*-test).

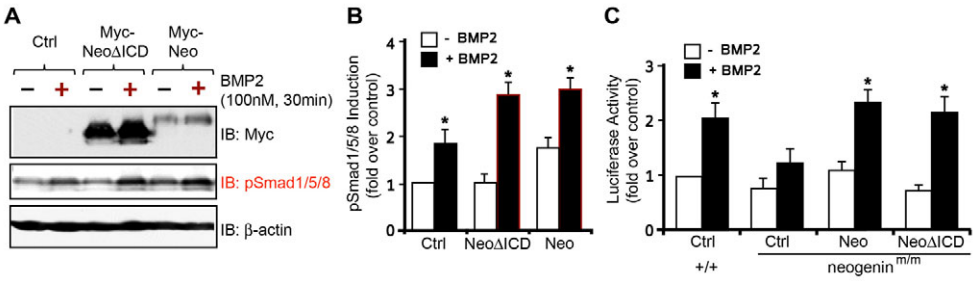

Fig. 6. Mouse neogenin lacking the intracellular domain is sufficient to mediate BMP signaling. (**A**) Western blot showing BMP2-induced pSmad1/5/8 in HEK293 cells expressing neogenin and neogeninΔICD. (**B**) Quantitative analysis of data from A. The levels of phosphorylation of Smad1/5/8 were quantified by ImageJ and normalized with the control. Data are mean ± s.d., $n=3$; *$P<0.05$ versus control (Student's t-test). (**C**) Rescue of defective BMP reporter expression by both neogenin and neogeninΔICD. Wild-type and neogenin mutant fibroblasts were transiently transfected with vector (control), neogenin, or neogeninΔICD plus the BMP signaling reporter plasmid (9XSBE-Luc). Two days after transfection, cells were stimulated with BMP2 (see Materials and methods). Luciferase activity was measured, normalized to the control without BMP2, and presented as mean ± s.d. of triplicates from a representative experiment. *$P<0.05$ versus the absence of BMP2 stimulation (Student's t-test).

proteins, and it has netrin-dependent roles in axon guidance, cell-cell adhesion and tissue organization (Srinivasan et al., 2003; Kang et al., 2004; Wilson and Key, 2006; Lejmi et al., 2008) and functions in BMP signaling (Zhang et al., 2009; Zhou et al., 2010). We have shown that, in addition to its previously reported roles in netrin-mediated axon guidance and cell migration, the single *C. elegans* DCC/neogenin homolog UNC-40 is capable of promoting BMP signaling by binding to the RGM protein DRAG-1. Importantly, these two functions of UNC-40 are independent of each other: (1) null mutations in genes that encode UNC-6/netrin and another netrin receptor, UNC-5, do not cause any defects in Sma/Mab signaling; (2) UNC-40 protein lacking the ICD is defective in netrin-mediated axon guidance and cell migration, but exhibits wild-type activity in Sma/Mab signaling; and (3) UNC-40 proteins lacking the sixth FNIII motif (FN6), or carrying mutations in the E-F loop of FN6, are defective in Sma/Mab signaling, but exhibit wild-type activity in netrin-mediated axon guidance and migration. Importantly, the role of UNC-40 in promoting Sma/Mab signaling requires its interaction with the RGM protein DRAG-1, which on its own does not appear to play any significant role in axon guidance and cell migration (our unpublished data). These findings suggest that, rather than acting as a convergent point between the netrin-mediated pathway and the BMP pathway, neogenin independently mediates these two pathways via distinct effectors. Although the ICD is clearly required for UNC-40/neogenin to mediate netrin signaling in axon guidance, it is dispensable for the role of UNC-40/neogenin in mediating BMP signaling. Consistently, the netrin-binding motif and the RGM-binding motif have been mapped to two independent regions of neogenin (Rajagopalan et al., 2004).

Our finding that the EXD of UNC-40 is sufficient to mediate BMP signaling suggests the intriguing possibility that UNC-40 might undergo proteolytic processing *in vivo* to release its EXD. In fact, both DCC and neogenin have previously been reported to undergo metalloprotease-mediated ectodomain shedding (Galko and Tessier-Lavigne, 2000; Okamura et al., 2011). Whether UNC-40 undergoes ectodomain shedding, and, if so, how this process is regulated spatially and temporally will be areas of future investigation.

A model for UNC-40/neogenin function in regulating BMP signaling

Results from our *in vitro* and *in vivo* experiments demonstrated that the EXD of UNC-40 binds to DRAG-1 and that this interaction is crucial for their function in Sma/Mab signaling. Moreover, both

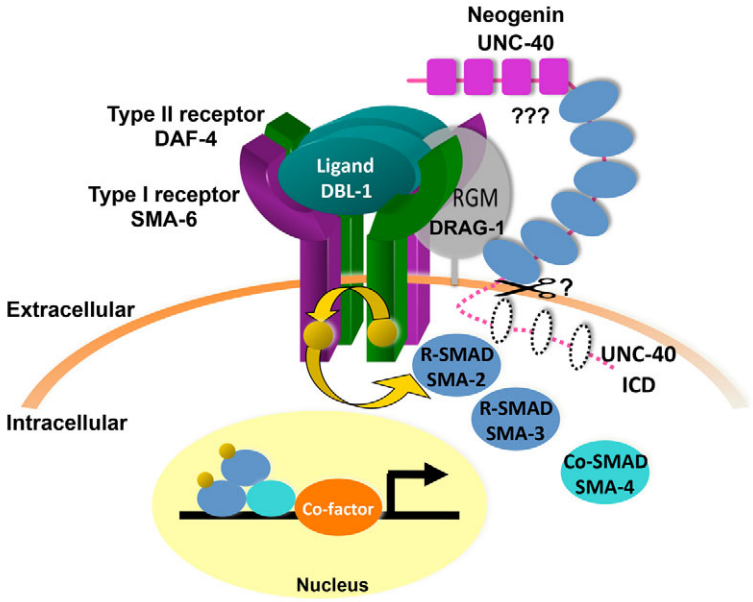

Fig. 7. A model of UNC-40 function in promoting BMP signaling. By interacting with DRAG-1 through its FN6 motif and through interactions with other, as yet unidentified, factors (???), UNC-40 allows an increased local concentration or stability of the ligand-receptor complex on the surface of the signal-receiving cell, thereby promoting Sma/Mab signaling. UNC-40 protein might be processed via 'ectodomain shedding'. The intracellular domain (ICD) of UNC-40 is depicted in dotted outline, as it is not required for Sma/Mab signaling. UNC-40 might also function in the signal-producing cells, which is not depicted here.

proteins function in *cis* in the same signal-receiving cells to promote BMP signaling (Tian et al., 2010) (this study). Because DRAG-1 binds to both the ligand and the receptors of the Sma/Mab pathway, we propose that the binding of UNC-40 to DRAG-1 might allow an increased local concentration or stability of the ligand/receptor complex, thereby promoting Sma/Mab signaling (Fig. 7). This is consistent with a model proposed by Zhou and colleagues in which neogenin positively modulates BMP signaling by promoting the formation of BMP-induced super-receptor complexes that include RGMs, neogenin and BMP receptors in membrane microdomains (Zhou et al., 2010).

DRAG-1, however, does not appear to be the only factor that interacts with UNC-40 to mediate its function in Sma/Mab signaling: (1) cell fractionation experiments showed that the EXD of UNC-40 is membrane associated and that this association is independent of DRAG-1 (data not shown); and (2) two additional *unc-40* alleles – *ev546*, which carries a G774R mutation in the FN4 motif (Alexander et al., 2010), and *tm5504*, which deletes the FN1 and FN2 motifs, exhibit incompletely penetrant SOSMLP phenotypes [12.16% (n=74) for *ev546* and 39.5% (n=215) for *tm5504*]. These FNIII motifs might be required for UNC-40 to interact with other components of the BMP pathway. Consistently, neogenin has been shown to directly bind to BMP ligand (Hagihara et al., 2011) but not BMP receptors (Zhou et al., 2010).

Future work will be directed towards identifying the other factors that interact with UNC-40 and how they function together to allow efficient BMP signaling. In light of the importance of the BMP pathway in regulating multiple developmental and homeostatic processes and the fact that mutations in RGMc cause JH, results from these studies are likely to have significant implications.

Acknowledgements
We thank the Caenorhabditis Genetics Center (CGC) (funded by the National Institutes of Health, Office of Research Infrastructure Programs P40 OD010440), Daniel Colon-Ramos, Joe Culotti, Eric Jorgensen, Keith Nehrke, Shohei Mitani, Peter Roy, Tarek Samad, Kang Shen, Stephen Strittmatter, William Wadsworth and Yimin Zou for strains and plasmids; Joe Culotti for sharing unpublished results; and Ken Kemphues, Mariana Wolfner and members of the J.L. lab for comments and suggestions.

Funding
This work was supported by grants from the National Institutes of Health [NIH GM066953 to J.L.; and NIH NS06648 to W.-C.X.] and from the Department of Veterans Affairs [VA BX00838 to W.-C.X.]. Deposited in PMC for release after 12 months.

Competing interests statement
The authors declare no competing financial interests.

Author contributions
C.T., H.S. and J.L. performed the experiments; S.X. performed the experiments presented in Fig. 6 under the supervision of W.-C.X.; F.H. provided reagents and contributed to discussion of the data; C.T. and J.L. conceived the project, designed the experiments, analyzed the data and wrote the manuscript.

Supplementary material
Supplementary material available online at
http://dev.biologists.org/lookup/suppl/doi:10.1242/dev.099838/-/DC1

References

Alexander, M., Chan, K. K., Byrne, A. B., Selman, G., Lee, T., Ono, J., Wong, E., Puckrin, R., Dixon, S. J. and Roy, P. J. (2009). An UNC-40 pathway directs postsynaptic membrane extension in Caenorhabditis elegans. *Development* **136**, 911-922.

Alexander, M., Selman, G., Seetharaman, A., Chan, K. K., D'Souza, S. A., Byrne, A. B. and Roy, P. J. (2010). MADD-2, a homolog of the Opitz syndrome protein MID1, regulates guidance to the midline through UNC-40 in Caenorhabditis elegans. *Dev. Cell* **18**, 961-972.

Allendorph, G. P., Vale, W. W. and Choe, S. (2006). Structure of the ternary signaling complex of a TGF-beta superfamily member. *Proc. Natl. Acad. Sci. USA* **103**, 7643-7648.

Amin, N. M., Hu, K., Pruyne, D., Terzic, D., Bretscher, A. and Liu, J. (2007). A Zn-finger/FH2-domain containing protein, FOZI-1, acts redundantly with CeMyoD to specify striated body wall muscle fates in the Caenorhabditis elegans postembryonic mesoderm. *Development* **1**, 19-29.

Babitt, J. L., Zhang, Y., Samad, T. A., Xia, Y., Tang, J., Campagna, J. A., Schneyer, A. L., Woolf, C. J. and Lin, H. Y. (2005). Repulsive guidance molecule (RGMa), a DRAGON homologue, is a bone morphogenetic protein co-receptor. *J. Biol. Chem.* **280**, 29820-29827.

Babitt, J. L., Huang, F. W., Wrighting, D. M., Xia, Y., Sidis, Y., Samad, T. A., Campagna, J. A., Chung, R. T., Schneyer, A. L., Woolf, C. J. et al. (2006). Bone morphogenetic protein signaling by hemojuvelin regulates hepcidin expression. *Nat. Genet.* **38**, 531-539.

Balemans, W. and Van Hul, W. (2002). Extracellular regulation of BMP signaling in vertebrates: a cocktail of modulators. *Dev. Biol.* **250**, 231-250.

Blelloch, R., Newman, C. and Kimble, J. (1999). Control of cell migration during Caenorhabditis elegans development. *Curr. Opin. Cell Biol.* **11**, 608-613.

Cai, J., Pardali, E., Sánchez-Duffhues, G. and ten Dijke, P. (2012). BMP signaling in vascular diseases. *FEBS Lett.* **586**, 1993-2002.

Chan, S. S., Zheng, H., Su, M. W., Wilk, R., Killeen, M. T., Hedgecock, E. M. and Culotti, J. G. (1996). UNC-40, a C. elegans homolog of DCC (Deleted in Colorectal Cancer), is required in motile cells responding to UNC-6 netrin cues. *Cell* **87**, 187-195.

Clark, S. G. and Chiu, C. (2003). C. elegans ZAG-1, a Zn-finger-homeodomain protein, regulates axonal development and neuronal differentiation. *Development* **130**, 3781-3794.

Colavita, A. and Culotti, J. G. (1998). Suppressors of ectopic UNC-5 growth cone steering identify eight genes involved in axon guidance in Caenorhabditis elegans. *Dev. Biol.* **194**, 72-85.

Cole, S. J., Bradford, D. and Cooper, H. M. (2007). Neogenin: a multi-functional receptor regulating diverse developmental processes. *Int. J. Biochem. Cell Biol.* **39**, 1569-1575.

Colón-Ramos, D. A., Margeta, M. A. and Shen, K. (2007). Glia promote local synaptogenesis through UNC-6 (netrin) signaling in C. elegans. *Science* **318**, 103-106.

Corradini, E., Babitt, J. L. and Lin, H. Y. (2009). The RGM/DRAGON family of BMP co-receptors. *Cytokine Growth Factor Rev.* **20**, 389-398.

Culotti, J. G. and Merz, D. C. (1998). DCC and netrins. *Curr. Opin. Cell Biol.* **10**, 609-613.

Estevez, M., Attisano, L., Wrana, J. L., Albert, P. S., Massagué, J. and Riddle, D. L. (1993). The daf-4 gene encodes a bone morphogenetic protein receptor controlling C. elegans dauer larva development. *Nature* **365**, 644-649.

Fire, A., Xu, S., Montgomery, M. K., Kostas, S. A., Driver, S. E. and Mello, C. C. (1998). Potent and specific genetic interference by double-stranded RNA in Caenorhabditis elegans. *Nature* **391**, 806-811.

Foehr, M. L., Lindy, A. S., Fairbank, R. C., Amin, N. M., Xu, M., Yanowitz, J., Fire, A. Z. and Liu, J. (2006). An antagonistic role for the C. elegans Schnurri homolog SMA-9 in modulating TGFbeta signaling during mesodermal patterning. *Development* **133**, 2887-2896.

Frøkjaer-Jensen, C., Davis, M. W., Hopkins, C. E., Newman, B. J., Thummel, J. M., Olesen, S. P., Grunnet, M. and Jorgensen, E. M. (2008). Single-copy insertion of transgenes in Caenorhabditis elegans. *Nat. Genet.* **40**, 1375-1383.

Galko, M. J. and Tessier-Lavigne, M. (2000). Function of an axonal chemoattractant modulated by metalloprotease activity. *Science* **289**, 1365-1367.

Gilleard, J. S., Shafi, Y., Barry, J. D. and McGhee, J. D. (1999). ELT-3: A Caenorhabditis elegans GATA factor expressed in the embryonic epidermis during morphogenesis. *Dev. Biol.* **208**, 265-280.

Gordon, K. J. and Blobe, G. C. (2008). Role of transforming growth factor-beta superfamily signaling pathways in human disease. *Biochim. Biophys. Acta* **1782**, 197-228.

Gumienny, T. L., MacNeil, L. T., Wang, H., de Bono, M., Wrana, J. L. and Padgett, R. W. (2007). Glypican LON-2 is a conserved negative regulator of BMP-like signaling in Caenorhabditis elegans. *Curr. Biol.* **17**, 159-164.

Hagihara, M., Endo, M., Hata, K., Higuchi, C., Takaoka, K., Yoshikawa, H. and Yamashita, T. (2011). Neogenin, a receptor for bone morphogenetic proteins. *J. Biol. Chem.* **286**, 5157-5165.

Harfe, B. D., Vaz Gomes, A., Kenyon, C., Liu, J., Krause, M. and Fire, A. (1998). Analysis of a Caenorhabditis elegans Twist homolog identifies conserved and divergent aspects of mesodermal patterning. *Genes Dev.* **12**, 2623-2635.

Hedgecock, E. M., Culotti, J. G. and Hall, D. H. (1990). The unc-5, unc-6, and unc-40 genes guide circumferential migrations of pioneer axons and mesodermal cells on the epidermis in C. elegans. *Neuron* **4**, 61-85.

Hong, K., Hinck, L., Nishiyama, M., Poo, M. M., Tessier-Lavigne, M. and Stein, E. (1999). A ligand-gated association between cytoplasmic domains of UNC5 and DCC family receptors converts netrin-induced growth cone attraction to repulsion. *Cell* **97**, 927-941.

Huang, F., and Chen, Y.G. (2012). Regulation of TGF-beta receptor activity. *Cell. Biosci.* **9**-3701-2-9.
Jiang, Y., Horner, V. and Liu, J. (2005). The HMX homeodomain protein MLS-2 regulates cleavage orientation, cell proliferation and cell fate specification in the C. elegans postembryonic mesoderm. *Development* **132**, 4119-4130.
Kang, J. S., Yi, M. J., Zhang, W., Feinleib, J. L., Cole, F. and Krauss, R. S. (2004). Netrins and neogenin promote myotube formation. *J. Cell Biol.* **167**, 493-504.
Keino-Masu, K., Masu, M., Hinck, L., Leonardo, E. D., Chan, S. S., Culotti, J. G. and Tessier-Lavigne, M. (1996). Deleted in Colorectal Cancer (DCC) encodes a netrin receptor. *Cell* **87**, 175-185.
Kennedy, T. E., Serafini, T., de la Torre, J. R. and Tessier-Lavigne, M. (1994). Netrins are diffusible chemotropic factors for commissural axons in the embryonic spinal cord. *Cell* **78**, 425-435.
Kramer, J. M. and Johnson, J. J. (1993). Analysis of mutations in the sqt-1 and rol-6 collagen genes of Caenorhabditis elegans. *Genetics* **135**, 1035-1045.
Krishna, S., Maduzia, L. L. and Padgett, R. W. (1999). Specificity of TGFbeta signaling is conferred by distinct type I receptors and their associated SMAD proteins in Caenorhabditis elegans. *Development* **126**, 251-260.
Kuns-Hashimoto, R., Kuninger, D., Nili, M. and Rotwein, P. (2008). Selective binding of RGMc/hemojuvelin, a key protein in systemic iron metabolism, to BMP-2 and neogenin. *Am. J. Physiol.* **294**, C994-C1003.
Lanzara, C., Roetto, A., Daraio, F., Rivard, S., Ficarella, R., Simard, H., Cox, T. M., Cazzola, M., Piperno, A., Gimenez-Roqueplo, A. P. et al. (2004). Spectrum of hemojuvelin gene mutations in 1q-linked juvenile hemochromatosis. *Blood* **103**, 4317-4321.
Lee, D. H., Zhou, L. J., Zhou, Z., Xie, J. X., Jung, J. U., Liu, Y., Xi, C. X., Mei, L. and Xiong, W. C. (2010). Neogenin inhibits HJV secretion and regulates BMP-induced hepcidin expression and iron homeostasis. *Blood* **115**, 3136-3145.
Lejmi, E., Leconte, L., Pédron-Mazoyer, S., Ropert, S., Raoul, W., Lavalette, S., Bouras, I., Feron, J. G., Maitre-Boube, M., Assayag, F. et al. (2008). Netrin-4 inhibits angiogenesis via binding to neogenin and recruitment of Unc5B. *Proc. Natl. Acad. Sci. USA* **105**, 12491-12496.
Maduro, M. and Pilgrim, D. (1995). Identification and cloning of unc-119, a gene expressed in the Caenorhabditis elegans nervous system. *Genetics* **141**, 977-988.
Maduzia, L. L., Gumienny, T. L., Zimmerman, C. M., Wang, H., Shetgiri, P., Krishna, S., Roberts, A. F. and Padgett, R. W. (2002). lon-1 regulates Caenorhabditis elegans body size downstream of the dbl-1 TGF beta signaling pathway. *Dev. Biol.* **246**, 418-428.
Massagué, J. (2008). TGFbeta in Cancer. *Cell* **134**, 215-230.
Morita, K., Chow, K. L. and Ueno, N. (1999). Regulation of body length and male tail ray pattern formation of Caenorhabditis elegans by a member of TGF-beta family. *Development* **126**, 1337-1347.
Morita, K., Flemming, A. J., Sugihara, Y., Mochii, M., Suzuki, Y., Yoshida, S., Wood, W. B., Kohara, Y., Leroi, A. M. and Ueno, N. (2002). A Caenorhabditis elegans TGF-beta, DBL-1, controls the expression of LON-1, a PR-related protein, that regulates polyploidization and body length. *EMBO J.* **21**, 1063-1073.
Okamura, Y., Kohmura, E. and Yamashita, T. (2011). TACE cleaves neogenin to desensitize cortical neurons to the repulsive guidance molecule. *Neurosci. Res.* **71**, 63-70.
Papanikolaou, G., Samuels, M. E., Ludwig, E. H., MacDonald, M. L., Franchini, P. L., Dubé, M. P., Andres, L., MacFarlane, J., Sakellaropoulos, N., Politou, M. et al. (2004). Mutations in HFE2 cause iron overload in chromosome 1q-linked juvenile hemochromatosis. *Nat. Genet.* **36**, 77-82.
Pettersen, E. F., Goddard, T. D., Huang, C. C., Couch, G. S., Greenblatt, D. M., Meng, E. C. and Ferrin, T. E. (2004). UCSF Chimera – a visualization system for exploratory research and analysis. *J. Comput. Chem.* **25**, 1605-1612.
Qin, S., Yu, L., Gao, Y., Zhou, R. and Zhang, C. (2007). Characterization of the receptors for axon guidance factor netrin-4 and identification of the binding domains. *Mol. Cell. Neurosci.* **34**, 243-250.
Quinn, C. C. and Wadsworth, W. G. (2008). Axon guidance: asymmetric signaling orients polarized outgrowth. *Trends Cell Biol.* **18**, 597-603.
Rajagopalan, S., Deitinghoff, L., Davis, D., Conrad, S., Skutella, T., Chedotal, A., Mueller, B. K. and Strittmatter, S. M. (2004). Neogenin mediates the action of repulsive guidance molecule. *Nat. Cell Biol.* **6**, 756-762.
Ramel, M. C. and Hill, C. S. (2012). Spatial regulation of BMP activity. *FEBS Lett.* **586**, 1929-1941.
Samad, T. A., Rebbapragada, A., Bell, E., Zhang, Y., Sidis, Y., Jeong, S. J., Campagna, J. A., Perusini, S., Fabrizio, D. A., Schneyer, A. L. et al. (2005). DRAGON, a bone morphogenetic protein co-receptor. *J. Biol. Chem.* **280**, 14122-14129.
Savage, C., Das, P., Finelli, A. L., Townsend, S. R., Sun, C. Y., Baird, S. E. and Padgett, R. W. (1996). Caenorhabditis elegans genes sma-2, sma-3, and sma-4 define a conserved family of transforming growth factor beta pathway components. *Proc. Natl. Acad. Sci. USA* **93**, 790-794.
Savage-Dunn, C. (2005). TGF-beta signaling. *WormBook* doi:10.1895.wormbook.1.22.1.
Severyn, C. J., Shinde, U. and Rotwein, P. (2009). Molecular biology, genetics and biochemistry of the repulsive guidance molecule family. *Biochem. J.* **422**, 393-403.
Shi, Y. and Massagué, J. (2003). Mechanisms of TGF-beta signaling from cell membrane to the nucleus. *Cell* **113**, 685-700.
Srinivasan, K., Strickland, P., Valdes, A., Shin, G. C. and Hinck, L. (2003). Netrin-1/neogenin interaction stabilizes multipotent progenitor cap cells during mammary gland morphogenesis. *Dev. Cell* **4**, 371-382.
Suzuki, Y., Yandell, M. D., Roy, P. J., Krishna, S., Savage-Dunn, C., Ross, R. M., Padgett, R. W. and Wood, W. B. (1999). A BMP homolog acts as a dose-dependent regulator of body size and male tail patterning in Caenorhabditis elegans. *Development* **126**, 241-250.
Teichmann, H. M. and Shen, K. (2011). UNC-6 and UNC-40 promote dendritic growth through PAR-4 in Caenorhabditis elegans neurons. *Nat. Neurosci.* **14**, 165-172.
Tian, C. and Liu, J. (2013). Repulsive guidance molecules (RGMs) and neogenin in bone morphogenetic protein (BMP) signaling. *Mol. Rep. Dev.* **9999**, 1-18.
Tian, C., Sen, D., Shi, H., Foehr, M. L., Plavskin, Y., Vatamaniuk, O. K. and Liu, J. (2010). The RGM protein DRAG-1 positively regulates a BMP-like signaling pathway in Caenorhabditis elegans. *Development* **137**, 2375-2384.
Umulis, D., O'Connor, M. B. and Blair, S. S. (2009). The extracellular regulation of bone morphogenetic protein signaling. *Development* **136**, 3715-3728.
Wadsworth, W. G., Bhatt, H. and Hedgecock, E. M. (1996). Neuroglia and pioneer neurons express UNC-6 to provide global and local netrin cues for guiding migrations in C. elegans. *Neuron* **16**, 35-46.
Wang, J., Tokarz, R. and Savage-Dunn, C. (2002). The expression of TGFbeta signal transducers in the hypodermis regulates body size in C. elegans. *Development* **129**, 4989-4998.
Wilson, N. H. and Key, B. (2006). Neogenin interacts with RGMa and netrin-1 to guide axons within the embryonic vertebrate forebrain. *Dev. Biol.* **296**, 485-498.
Wilson, N. H. and Key, B. (2007). Neogenin: one receptor, many functions. *Int. J. Biochem. Cell Biol.* **39**, 874-878.
Wu, M. Y. and Hill, C. S. (2009). Tgf-beta superfamily signaling in embryonic development and homeostasis. *Dev. Cell* **16**, 329-343.
Yamashita, T., Mueller, B. K. and Hata, K. (2007). Neogenin and repulsive guidance molecule signaling in the central nervous system. *Curr. Opin. Neurobiol.* **17**, 29-34.
Yang, F., West, A. P., Jr, Allendorph, G. P., Choe, S. and Bjorkman, P. J. (2008). Neogenin interacts with hemojuvelin through its two membrane-proximal fibronectin type III domains. *Biochemistry* **47**, 4237-4245.
Yang, F., West, A. P., Jr and Bjorkman, P. J. (2011). Crystal structure of a hemojuvelin-binding fragment of neogenin at 1.8Å. *J. Struct. Biol.* **174**, 239-244.
Yoshida, S., Morita, K., Mochii, M. and Ueno, N. (2001). Hypodermal expression of Caenorhabditis elegans TGF-beta type I receptor SMA-6 is essential for the growth and maintenance of body length. *Dev. Biol.* **240**, 32-45.
Zhang, A. S., West, A. P., Jr, Wyman, A. E., Bjorkman, P. J. and Enns, C. A. (2005). Interaction of hemojuvelin with neogenin results in iron accumulation in human embryonic kidney 293 cells. *J. Biol. Chem.* **280**, 33885-33894.
Zhang, A. S., Anderson, S. A., Meyers, K. R., Hernandez, C., Eisenstein, R. S. and Enns, C. A. (2007). Evidence that inhibition of hemojuvelin shedding in response to iron is mediated through neogenin. *J. Biol. Chem.* **282**, 12547-12556.
Zhang, A. S., Yang, F., Wang, J., Tsukamoto, H. and Enns, C. A. (2009). Hemojuvelin-neogenin interaction is required for bone morphogenic protein-4-induced hepcidin expression. *J. Biol. Chem.* **284**, 22580-22589.
Zhou, Z., Xie, J., Lee, D., Liu, Y., Jung, J., Zhou, L., Xiong, S., Mei, L. and Xiong, W. C. (2010). Neogenin regulation of BMP-induced canonical Smad signaling and endochondral bone formation. *Dev. Cell* **19**, 90-102.

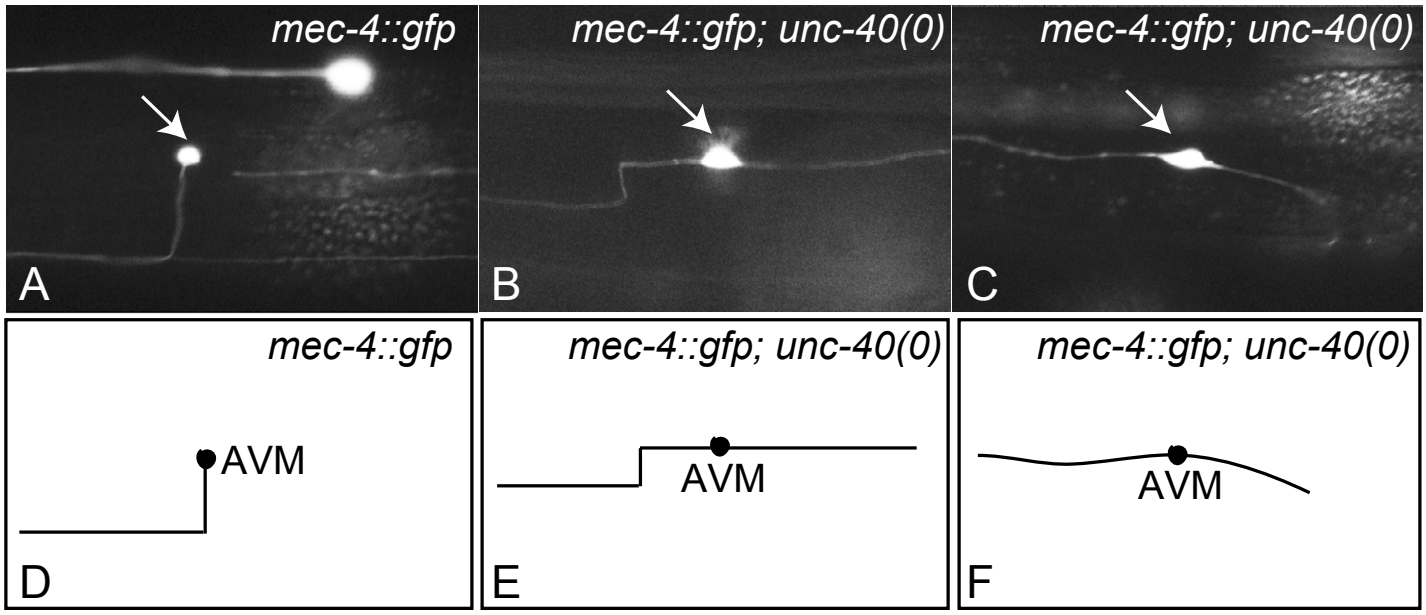

Fig. S1. The AVM migration defects of *unc-40* mutants. Photomicrographs (**A-C**) and corresponding schematics (**D-F**) of animals showing the AVM cell body (arrow) and axon projections as marked by *mec-4::gfp*. Anterior is to the left and dorsal is up. In wild-type animals (A,D), the AVM axon first migrates ventrally and then turns anteriorly to migrate along the ventral nerve cord. (B,C,E,F) Examples of AVM axon migration defects in *unc-40* mutants.

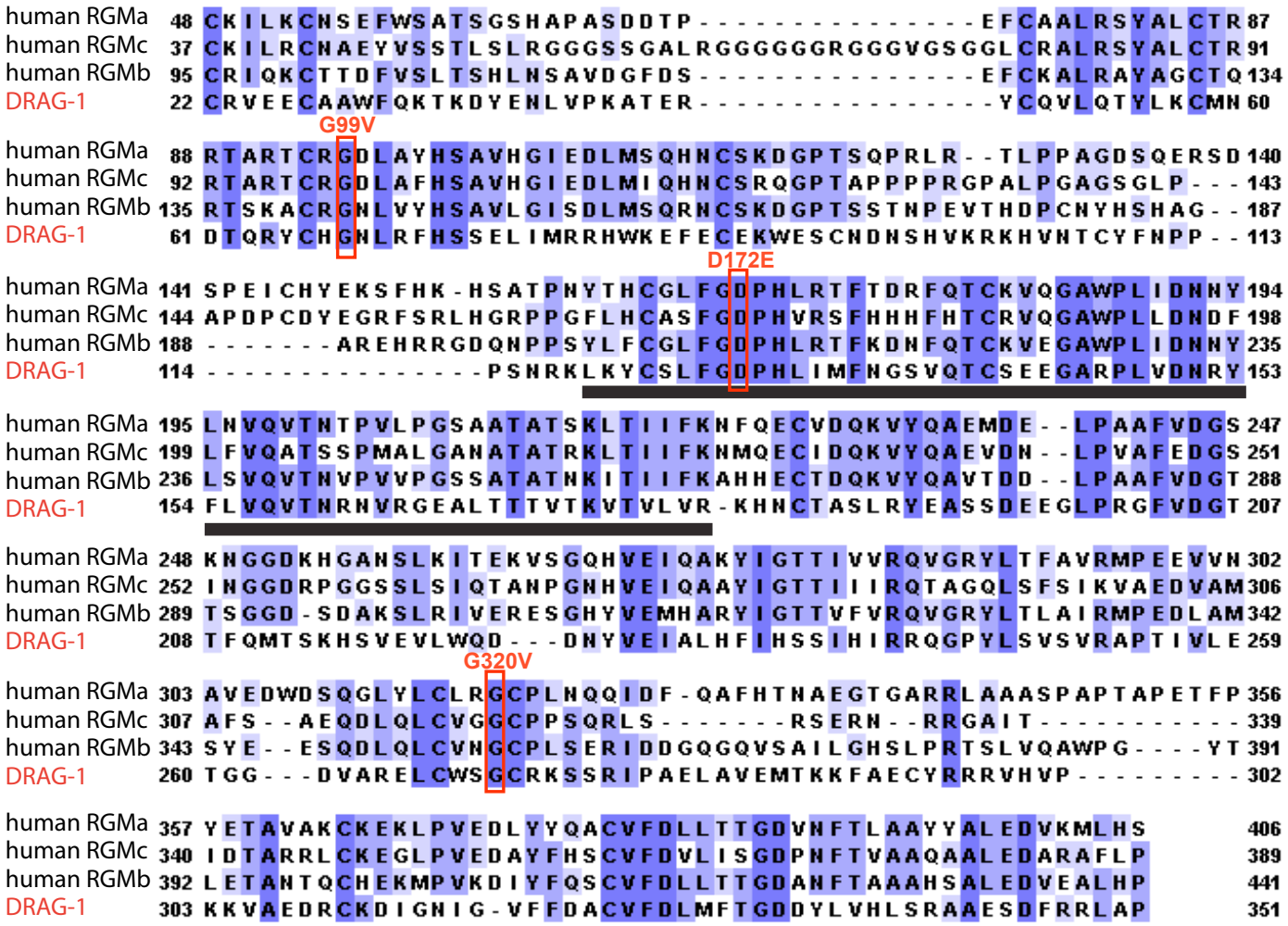

Fig. S2. DRAG-1 shares conserved features with human RGM proteins. Sequence comparison between mature human RGMa, RGMb and RGMc (HFE2) and *C. elegans* DRAG-1 proteins, highlighting conserved residues (blue). The N- and C-terminal signal sequences are not shown. The black line underlines the partial vWF type D domain. The three JH (juvenile hemochromatosis) disease-associated hypomorphic mutations discussed in this paper are boxed in red (Lanzara et al., 2004).

Table S1. Plasmid constructs

Constructs for tissue-specific expression of *unc-40*
pCXT261, unc-40p::unc-40 cDNA::gfp::unc-54 3'UTR
pCXT262, elt-3p::unc-40 cDNA::gfp::unc-54 3'UTR
pCXT264, rol-6p::unc-40 cDNA::gfp::unc-54 3'UTR
pCXT266, hlh-8p::unc-40cDNA::gfp::unc-54 3'UTR
pCXT265, unc-119p::unc-40cDNA::gfp::unc-54 3'UTR
pCXT289, myo-3p::unc-40 cDNA::gfp::unc-54 3'UTR
Mammalian cell culture expression constructs (all cloned into the pSecTag vector)
pCXT239 (DRAG-1-FLAG), *pCMV::signal peptide::DRAG-1 mature region (aa22-360)::FLAG*
pJKL962 (Myc-DRAG-1), *pCMV::signal peptide::cMyc-His::DRAG-1 mature region (aa22-360)*
pCXT271 (DRAG-1^{G272V}-FLAG), *pCMV::signal peptide::DRAG-1 mature region (aa22-360)^{G272V}::FLAG*
pCXT245 (Myc-FN5,6), *pCMV::signal peptide::cMyc-His-UNC-40 FNIII 5-6 (aa852-1081)*
pCXT249(Myc-FN5,6 C-C'loop), *pCMV::signal peptide::cMyc-His-UNC-40 FNIII 5-6 (aa852-1081) with aa987-993 mutated from DRASLAD to LDKNIPI*
pCXT299 (Myc-FN5,6 C'strand), *pCMV::signal peptide::cMyc-His-UNC-40 FNIII 5-6 (aa852-1081) with aa997-1002 mutated from TINYVA to IMETIS*
pCXT300 (Myc-FN5,6 E-Floop), *pCMV::signal peptide::cMyc-His-UNC-40 FNIII 5-6 (aa852-1081) with aa1011-1014 mutated from SNLL to MDLN*
pJKL964 (Myc-SMA-6), *pCMV::signal peptide::cMyc-His-SMA-6 full length (aa27–stop)*
pCXT230 (Myc-DAF-4), *pCMV::signal sequence::cMyc-His-DAF-4 EXD- TM-partial ICD (aa33–468)*
pCXT241 (FLAG-DBL-1), *pCMV::signal sequence::DBL-1 prodomain (aa32-238)::FLAG-DBL-1 mature region (aa239–stop)*
Constructs for making DRAG-1 and UNC-40 vertebrate and *C. elegans* hybrids
pCXT161, *drag-1p (–3977 to –1 and 4 to 1123)::drag-1 signal sequence:: mRgmb mature region::drag-1 C-signal sequence::unc-54 3'UTR*, has aa23-375 of DRAG-1 replaced by aa59-414 of mouse Rgmb in pCXT15 (Tian et al., 2010)
pCXT185, *drag-1p (–3977 to –1 and 4 to 1123)::drag-1 signal sequence:: hHJV mature region::drag-1 C-signal sequence::unc-54 3'UTR*, has aa23-375 of DRAG-1 replaced by aa38-398 of human RGMc/HJV in pCXT15
pCXT278, *unc-40p (–610 to –1)::unc-40 signal sequence::mDCC mature region::unc-54 3'UTR*, has aa36-stop of UNC-40 replaced by aa34-stop of mDCC
pCXT279, *unc-40p (–610 to –1)::unc-40 signal sequence::mNeo1 mature region::unc-54 3'UTR*, has aa36-stop of UNC-40 replaced by aa58-stop of mouse Neo1
Constructs for *in vivo* structure-function analysis of UNC-40 All constructs are derived from pZF22, a functional *unc-40::gfp* fusion described by Chan et al. (Chan et al., 1996)
pCXT253(ΔFN5), *unc-40::gfp without aa852-939*
pCXT254(ΔFN6), *unc-40::gfp without aa946-1041*
pCXT255(ΔFN5,6), *unc-40::gfp without aa852-1041*
pCXT260 (UNC-40 EXD), *unc-40 (aa1-1079)::gfp*
pCXT269(UNC-40 C-C' loop), *unc-40::gfp with aa987-993 mutated from DRASLAD to LDKNIPI*
pCXT285(UNC-40 C' strand), *unc-40::gfp with aa997-1002 mutated from TINYVA to IMETIS*
pCXT286(UNC-40 E-F loop), *unc-40::gfp with aa1011-1014 mutated from SNLL to MDLN*
Constructs for expressing wild-type and mutant *drag-1* using the MosSCI technique
pCXT208: *wildtype DRAG-1 in pCFJ151*
pCXT224: *DRAG-1G68V (GGT to GTT) in pCFJ151*
pCXT225: *DRAG-1D117E (GAT to GAA) in pCFJ151*
pCXT223: *DRAG-1G272V (GGA to GTA) in pCFJ151*